

Iron line in the afterglow: a key to the progenitor

D. Lazzati¹, G. Ghisellini and S. Campana

Osservatorio Astronomico di Brera, via E. Bianchi 46, I-23807 Merate (LC), Italy

Abstract. The discovery of a powerful and transient iron line feature in the X-ray afterglow spectrum of GRB 970508 and GRB 970828, if confirmed, would be a major breakthrough for understanding the nature the progenitor of gamma-ray bursts. We show that a large mass of iron very close to the burster is necessary to produce the emission line. This in itself strongly limits the possible progenitor of the gamma-ray event, suggesting the former explosion of a supernova, as predicted in the Supernova model (Vietri & Stella 1998). The line emission process and the line intensity depend strongly on the age, density and temperature of the remnant. The simultaneous observation of the iron line and of a power-law optical afterglow lasted for one year strongly suggest that the burst emission is isotropic. Recent observations of GRB 990123 are also discussed.

1. Introduction

Piro et al. (1999) and Yoshida et al. (1999) report the detection of an iron emission line feature in the X-ray afterglow spectra of GRB 970508 and GRB 970828, respectively. Both lines are characterized by a large flux and equivalent width (EW) compared with the theoretical previsions made in the framework of the hypernova and compact merger GRB progenitor models (Ghisellini et al. 1999, Böttcher et al. 1999). The line detected in GRB 970508 is consistent with an iron K_{α} line redshifted to the rest-frame of the candidate host galaxy ($z = 0.835$, Metzger et al. 1997), while GRB 970828 has no measured redshift and the identification of the feature with the same line would imply a redshift $z \sim 0.33$. The line fluxes (equivalent widths) are $F_{Fe} = (2.8 \pm 1.1) \times 10^{-13}$ erg cm $^{-2}$ s $^{-1}$ (EW ~ 1 keV) and $F_{Fe} = (1.5 \pm 0.8) \times 10^{-13}$ erg cm $^{-2}$ s $^{-1}$ (EW ~ 3 keV) for GRB 970508 and GRB 970828, respectively. As indicated by the flux uncertainties, these line features are revealed at a statistical level of $\sim 3\sigma$. A strong iron emission line unambiguously points towards the presence, in the vicinity of the burster, of a few per cent of iron solar masses concentrated in a compact region. Thus the presence of such a line in the X-ray afterglow spectrum would represent the “Rosetta Stone” for unveiling the burst progenitor.

¹Dipartimento di Fisica, Università degli studi di Milano, via Celoria 16, I-20133 Milano, Italy

To date, three main classes of models have been proposed for the origin of gamma-ray bursts (GRB): neutron star – neutron star (NS–NS) mergers (Paczyński 1986; Eichler et al. 1989), Hypernovae or failed type Ib supernovae (Woosley 1993; Paczyński 1998) and Supranovae (Vietri & Stella 1998). In the NS–NS model the burst is produced during the collapse of a binary system composed of two neutron stars or of a neutron star and a black hole. Interacting neutrinos or the spin–down of the remnant black hole should power a relativistic outflow and, eventually, the production of γ –ray photons. Hypernovae are the final evolutionary stage of very massive stars ($M \sim 100 M_\odot$), whose core implodes in a black hole without the explosion of a classical supernova. Again, the rotational energy of the remnant black hole is tapped by a huge magnetic field, powering the burst explosion. While NS–NS mergers should take place outside the original star formation site, due to the large peculiar velocities and long lifetime of the coalescing binary systems, hypernovae take place in the dense and possibly iron rich molecular cloud where the massive star was born.

The Supernova scenario (Vietri & Stella 1998) assumes that, following a supernova explosion, a fast spinning neutron star is formed, with a mass that would be supercritical in the absence of rotation. As radiative energy losses spin it down in a time–scale of months to years, it inevitably collapses to a Kerr black hole, whose rotational energy can then power the GRB. A supernova remnant (SNR) is naturally left over around the burst location.

2. Mass, size and shape of the surrounding material

Since the detected lines are both characterized by a flux of several $10^{-13} \text{ erg s}^{-1}$, we adopt as reference a line with a flux¹ $F_{Fe} = 10^{-13} F_{Fe,-13} \text{ erg cm}^{-2} \text{ s}^{-1}$.

This in itself constrains both the amount of line–emitting matter and the size of the emitting region.

We assume that the emitting region is a homogeneous spherical shell centered in the GRB progenitor, with radius R and width $\Delta R \leq R$. A limit to the size of the emitting region can be set, *independently from the flux variability*, imposing the flux level times the minimum duration of the emission (R/c) to be less than the total available energy supplied by the burst fluence. Allowing for an efficiency q of the burst photon reprocessing into the line ($q < 0.1$, see Ghisellini et al. 1999) we have:

$$R < 3 \times 10^{17} q^{-1} \frac{\mathcal{F}_{-5}}{F_{Fe,-13}} \text{ cm} \quad (1)$$

where \mathcal{F} is the total GRB fluence. Note that this result, obtained with independent arguments, agrees with the ~ 1 day variability time–scales of the detected features.

To obtain a lower limit to the total amount of mass (see Lazzati et al. 1999) we consider a parameter k given by the ratio between the total number of iron line photons divided by the number of iron nuclei: k is the number of photons produced by a single iron atom. This number can be constrained to be less than

¹Here and in the following we parametrise a quantity Q as $Q = 10^x Q_x$ and adopt cgs units.

the total number of ionizations an ion can undergo when illuminated by the burst or X-ray afterglow photons. For a GRB located at $z = 1$, we obtain²:

$$k \lesssim \frac{q E}{4\pi \epsilon_{ion} R^2} \sigma_K = 6.5 \times 10^6 \frac{q E_{52}}{R_{16}^2} \quad (2)$$

where E is the total energy of the burst photons, ϵ_{ion} the energy of an ionizing photon and σ_K the ionization cross-section of the iron K shell. The total mass is given by the ratio of the total number of produced photons divided by k times the mass of the iron atom. We have:

$$M \gtrsim 0.13 \frac{F_{Fe,-13} t_5 R_{16}^2}{q_{-1} A_{\odot} E_{52}} M_{\odot} \quad (3)$$

where t_5 is the time during which the line is observed in units of 10^5 seconds and A_{\odot} is the iron abundance in solar units.

If such a large amount of mass were uniformly spread around the burst location, it would completely stop the fireball. In fact (see e.g. Wijers, Rees & Mészáros 1997) the fireball is slowed down to sub-relativistic speeds when the swept up mass equals its initial rest mass. With a typical baryon load of $\sim 10^{-(4 \div 6)} M_{\odot}$, the mass predicted in Eq. 3 would stop the fireball after an observer time $t \sim \Gamma^{-2} R/c \sim 3 \times 10^4 \Gamma_1^{-2}$ s, i.e. almost one day. Any surviving long wavelength emission should then decay exponentially in the absence of energy supply. The only way to reconcile a monthly lasting power-law optical afterglow with iron line emission is through a particular geometry, in which the line of sight is devoid of the remnant matter. This implies (see also Fig. 1) that the burst emission is only moderately (if at all) beamed, since the burst photons must illuminate the surrounding matter and the line of sight simultaneously.

3. Emission mechanisms

The limits on the mass discussed in the above section are very general and independent of the mechanism producing the line photons. Lazzati et al. 1999 give a complete analysis of three mechanisms that are able to generate such an intense line feature.

Recombination In this scenario, burst (or X-ray afterglow) photons keep all the iron in the vicinity of the burst fully ionized. If the density of iron and free electrons is large and the plasma is cool, recombination of free electrons with iron nuclei is efficient and iron line photons are produced. However, we require that both $n_{Fe} \gtrsim 10^{10} \text{ cm}^{-3}$ and that $T \lesssim 10^4 \text{ K}$. During the burst Inverse Compton interactions of free electrons with γ -ray photons heat the plasma to $T \sim 10^8 \text{ K}$, and recombination is inefficient. This scenario may, however, be marginally consistent with GRB 970508 data if the ionization flux is provided by an afterglow with a high energy tail but with typical Compton temperature of $T_C \sim 10^{4 \div 5} \text{ K}$.

²The cosmological parameters will be set throughout this paper to $H_0 = 65 \text{ km s}^{-1} \text{ Mpc}^{-1}$, $q_0 = 0.5$ and $\Lambda = 0$.

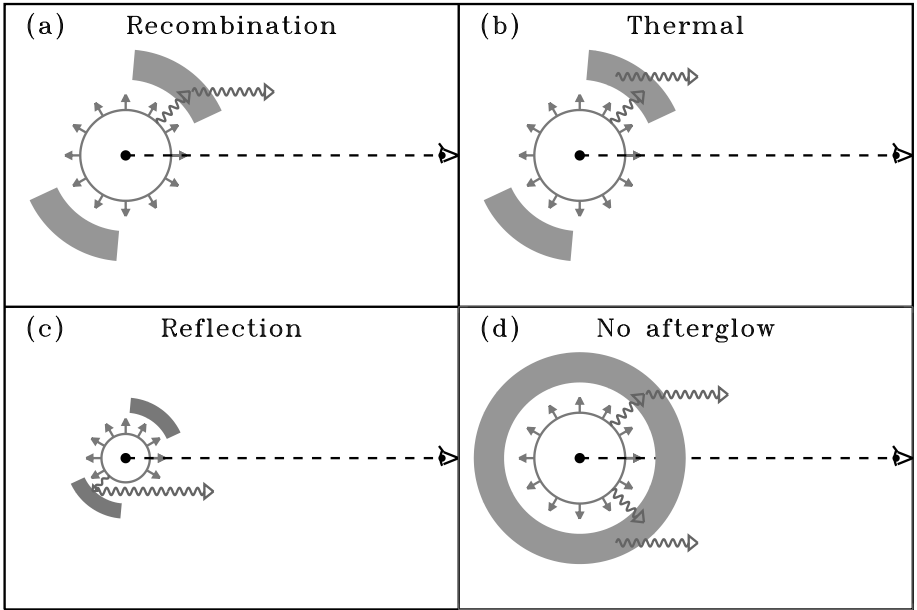


Figure 1. Cartoon illustrating the different emission mechanisms discussed in this paper. Shaded regions represent the supernova remnant, circles (with arrows) represent the fireball. In a) photons from the bursts photoionize iron atoms in the remnant shell, which recombine many times during the burst. In b) the shell has been heated by the burst photons, and emits thermally. In c) the shell, more compact than in the other cases, produces an iron fluorescent line, and a Compton reflection continuum. The last panel d) shows that if the remnant has a covering factor of unity, there should be no standard afterglow emission, since the fireball is suddenly stopped by the remnant.

Thermal emission A supernova remnant of several solar masses, some months after the explosion of the supernova, has an emission integral of the same order of magnitude of the intergalactic medium of a galaxy cluster. These systems emit 6.7 keV iron lines due to collisional excitation of hydrogenoid iron ions. In addition, the iron richness of a supernova remnant can be up to ten times larger than in a cluster of galaxies, allowing for the emission of iron line with several keV equivalent widths. In addition to the line, the heated SNR produces bremsstrahlung radiation at a level $F_{ff} \sim 10^{-13} \text{ erg cm}^{-2} \text{ s}^{-1}$, compatible with a standard X-ray afterglow at $z \sim 1$.

Reflection If some dense matter (e.g. a SNR with less than a month of life) is present in close vicinity with the burster, part of the incident radiation is reflected toward the observer. This same physical process is efficient in the disc of Seyfert galaxies, and a strong iron line is produced since the cross section of the iron atom is much larger than that of free electrons. For a $z \sim 1$ burst, lines with up to $F_{Fe} \sim 10^{-13} \text{ erg cm}^{-2} \text{ s}^{-1}$ can be produced. In steady state, $\sim 150 \text{ eV EW}$ lines are produced (if the material covers half of the sky), but in gamma-ray bursts the reflected component is seen when the burst emission has

already faded and the EW can be much higher (even a few keV). Given the fast variability properties of the detected lines, this model is favored with respect to recombination and thermal emission.

4. Progenitor

The presence of dense matter at rest in the reference frame of the burster (and not of the fireball) is a discriminating parameter for the main models of burst progenitor. Here we analyze the two main models, binary neutron star mergers and hypernovae, and a particular model, the Supranova, that naturally accounts for the surrounding iron rich matter.

The production of lines in the fireball has been discussed in Mészáros & Rees 1998a. They find that lines (particularly iron lines) can be produced inside the fireball, but we should observe them at a frequency $\nu_{obs} = \Gamma/(1+z)\nu_l$, where ν_l is the frequency of the line in the laboratory. In the case of GRB 970508 the observed frequency of the line is consistent with an iron line at the same redshift of the burster. An incredible fine-tuning is necessary to explain the feature as an optical–UV line blueshifted in the X-ray band due to the fireball expansion.

The line must hence be produced by the interaction of the burst photons with cold matter that surrounds the burster.

Binary compact object mergers The lifetime of a binary system composed of a couple of compact objects (NS–NS or BH–NS) ranges from 100 million to 10 billion years, mainly depending on the initial separation and on the mass of the binary system components (see e.g. Lipunov et al 1995). Due to the kick velocity that a compact object inherits from the supernova explosion that generated it, $\sim 200 \text{ km s}^{-1}$ on average (Kalogera et al. 1998), these binary systems merge well outside their formation site and, possibly, even outside the host galaxy. Assuming an hydrogen density $n = 1 \text{ cm}^{-3}$ and a solar iron abundance, a sphere of radius:

$$R \gtrsim 3.7 \times 10^{23} n^{-1} \frac{F_{Fe,-13} t_5}{q-1 A_\odot E_{52}} \text{ cm} \quad (4)$$

is necessary to meet the requirements of Eq. 3. However, the radius of the above equation is five orders of magnitude larger than the maximum allowed value (cf. Eq. 1).

Hypernova If we insert in Eq. 4 the density appropriate for a molecular cloud, in which a very massive star is thought to be located, we obtain $R \sim 3 \times 10^{18} A_\odot^{-1} \text{ cm}$ for $n = 10^5 \text{ cm}^{-3}$ that, for an iron rich cloud, is marginally consistent with the limit of Eq. 1. To firmly rule out the possibility of an intense iron line produced in the hypernova scenario, we analyze each emission mechanism discussed in Sect. 3.. Reflection can be immediately excluded since a radius $R > 10^{20} \text{ cm}$ cloud is necessary to have a Thomson thick mirror. The efficiency of thermal emission is proportional to the square of the density. Lazzati et al. 1999 estimate that both a density $n \sim 10^{10} \text{ cm}^{-3}$ and a mass of several solar masses (see also Sect. 3.) are necessary to produce such an intense iron line. In the hypernova scenario, the density is 5 orders of magnitude smaller, giving a flux 10 orders of magnitude fainter. The recombination time in a medium

with the considered density is too long (see Böttcher et al. 1999), however a fluorescence line may be emitted due to ionization of the inner shell of almost neutral iron atoms. The more optimistic estimate of the line flux produced by fluorescence in a molecular cloud is given in Ghisellini et al. 1999, with an upper limit $F_{Fe} < 5 \times 10^{-15}$ erg cm $^{-2}$ s $^{-1}$. Even if we consider the presence of a pre-hypernova wind with $\dot{m} \sim 10^{-4} M_{\odot}$ /yr, the total mass contained in a radius of 10^{18} cm would be a few percent of a solar mass, leaving the above discussion unaffected. We hence conclude that in a standard hypernova scenario it is not possible to produce an intense iron line.

Mészáros & Rees 1998b discussed the possible production of an intense iron line if a compact companion of the hypernova has left a dense torus of material ($M \sim M_{\odot}$; $n \sim 10^{10}$ cm $^{-3}$) at a distance $R \sim 10^{15}$ cm from the burster. Another progenitor model can account for this matter in a more natural way.

5. Supranova

In the model presented by Vietri & Stella 1998 the burst explosion is preceded by a supernova. The neutron star left over by the supernova explosion is supermassive, i.e. its mass exceeds the limiting mass for a neutron star, but the implosion in a black hole is prevented by the fast rotation. As the system spins down, due to radiative losses, the neutron star shrinks until a limiting state is reached and the star collapses in a black hole. The duration of this transient phase depends from the strength of the magnetic field embedded in the star and from the initial spin velocity, but should typically last between several months and a dozen of years. If we consider a supernova exploded a year before the burst, the density of its shell remnant at the burst onset is:

$$n \sim 5 \times 10^9 M_{\odot} v_9^3 \text{ cm}^{-3} \quad (5)$$

where M_{\odot} is the mass of the ejecta in solar units, v_9 is their speed in units of 10^9 cm s $^{-1}$ and the width of the shell has been assumed $\Delta R = R/100$. The shell radius is $R = 3 \times 10^{16}$ cm, in good agreement with the constraints derived above. If we consider that a SNR can have an iron richness ten times the solar value (Woosley 1988), this scenario is the most natural one to explain the intense iron line observed in the afterglow of GRB 970508 and GRB 970828.

6. GRB 990123

The recent explosion of GRB 990123 has gathered the attention of the gamma-ray astronomers due to the huge fluence and large distance of this burst. The early X-ray afterglow flux was measured by the *Beppo-SAX* satellite at a level of $F \sim 1.1 \times 10^{-11}$ erg s $^{-1}$ (Heise et al. 1999) about 6 hours after the burst trigger. The first results on the spectral analysis gives a “featureless spectrum” (Heise et al. 1999). If an iron line feature with the same EW of those of GRB 970508 and GRB 970828 were present in the afterglow of GRB 990123, a firm detection would have been established: since the underlying continuum flux of the latter burst is ~ 100 times larger than in the other two cases, the signal to noise ratio of the line would have been 10 times larger. Moreover, due to the larger redshift

of GRB 990123 (z=1.6004, Kulkarni et al. 1999) the redshifted line energy lies in a region where the detector efficiency is the largest. This could have led to a 30σ line feature.

There are, however, two reasons why an iron line is not expected in the afterglow of GRB 990123. First, (Lazzati et al. 1999) the line intensity is limited by the recombination time and not by the ionization time. This means that, even in the case of GRB 970508 - a weak burst - the ionizing flux was more than enough to fully exploit the matter surrounding the progenitor. If an iron line with flux $F_{Fe} \sim 3 \times 10^{-13} \text{ erg cm}^{-2} \text{ s}^{-1}$ was present in the X-ray afterglow of the 23 January burst, its EW would be decreased to the very low value of $\sim 10 \text{ eV}$, hence well below the detection threshold of the *Beppo-SAX*. Finally, the break in the power-law decrease of the optical light curve of GRB 990123 afterglow has been interpreted as a sign of beaming in the burst itself (Kulkarni et al. 1999; Fruchter et al 1999). If this interpretation is correct, even if a cloud were present in close vicinity with the burster, its illumination would have been minimal, preventing the formation of an intense line.

7. Discussion

We have analyzed how the detection of an iron line redshifted to the rest frame of the burster can be used to constrain the progenitor models. Indeed, due to the relativistic outflows involved in the fireball model, very poor information of the progenitor is contained in the gamma-ray burst photons, and the only mean to investigate the progenitor nature is through the interaction of the photons with the ambient medium.

In particular, we have analyzed three different models predicting very different conditions of the external medium: the merging of two compact objects in a binary system, the hypernova and the Supernova. We derived a (model-independent) lower limit to the mass required to produce the line, ruling out the NS-NS merger model and, with a careful analysis, the hypernova. The Supernova, which naturally accounts for a shell remnant of iron rich material surrounding the burster seems the most promising model capable to produce an intense iron line.

Due to the paucity of the statistical significance of the line detections, more observations are needed to draw firm conclusions. We show that, despite its luminosity, GRB 990123 is not the ideal test for the line detection and more observations with more efficient satellites are needed.

Acknowledgments. DL thanks the Cariplo foundation for financial support.

References

Böttcher, M., Dermer, C. D., Crider, A. W., & Liang, E. P. 1999, A&A, 343, 111
 Eichler, D., Livio, M., Piran, T., & Shramm, D. N. 1989, Nature, 340, 126
 Fruchter A. S., et al. 1999, ApJ submitted (astro-ph/9902236)
 Heise, J., et al. 1999, IAUC n. 7099

Kalogera, V., Kolb, U., & King, A. R. 1998, *ApJ*, 504, 967
Kulkarni, S., et al. 1999, *Nature*, 398, 389
Lazzati, D., Campana, S., & Ghisellini, G. 1999, *MNRAS*, 304, L31
Lipunov, V. M., Postnov, K. A., Prokhorov, M. E., & Panchenlo, I. E. 1995,
ApJ, 454, 593
Mészáros, P., & Rees, M. J. 1998a, *ApJ*, 502, L105
Mészáros, P., & Rees, M. J. 1998b, *MNRAS*, 299, L10
Metzger, M. R., et al. 1997, *Nature*, 387, 878
Paczyński, B. 1986, *ApJ*, 308, L43
Paczyński, B. 1998, *ApJ*, 494, L45
Piro, L., et al. 1999, *ApJ*, 514, L73
Vietri, M., & Stella. L. 1998, *ApJ*, 507, L45
Wijers, R. A. M. J., Rees, M. J., & Mészáros, P. 1997, *MNRAS*, 288, L51
Woosley, S. E. 1988, *ApJ*, 330, 218
Woosley, S. E. 1993, *ApJ*, 405, 273
Yoshida, A., et al. 1999, *ApJ* in press